H_2-driven xylitol production in *Cupriavidus necator* H16

Tytti Jämsä[1,*] ID, Nico J. Claassens[2] ID, Laura Salusjärvi[1] ID, Antti Nyyssölä[1] ID

Abstract

Background: Biocatalysis offers a potentially greener alternative to chemical processes. For biocatalytic systems requiring cofactor recycling, hydrogen emerges as an attractive reducing agent. Hydrogen is attractive because all the electrons can be fully transferred to the product, and it can be efficiently produced from water using renewable electricity. In this article, resting cells of *Cupriavidus necator* H16 harboring a NAD-dependent hydrogenase were employed for cofactor recycling to reduce D-xylose to xylitol, a commonly used sweetener. To enable this bioconversion, D-xylose reductase from *Scheffersomyces stipitis* was heterologously expressed in *C. necator*.

Results: D-xylose reductase was successfully expressed in *C. necator*, enabling complete bioconversion of 30 g/L of D-xylose into xylitol within 7 days using resting cells. It was found that over 90% of the energy and protons derived from hydrogen were spent for the bioconversion, demonstrating the efficiency of the system. The highest xylitol productivity reached was 0.7 g L^{-1} h^{-1}. Additionally, the same chassis efficiently produced L-arabitol and D-ribitol from L-arabinose and D-ribose, respectively.

Conclusions: This study highlights the efficient utilization of renewable hydrogen as a reducing agent to power cofactor recycling. Hydrogen-oxidizing bacteria, such as *C. necator*, can be promising hosts for performing hydrogen-driven biocatalysis.

Affiliations

[1] VTT Technical Research Centre of Finland Ltd., Tekniikantie 21, 02150 Espoo, Finland

[2] Laboratory of Microbiology, Wageningen University, Stippeneng 4, 6708WE Wageningen, the Netherlands

*Corresponding author E-mail address: tytti.jamsa@vtt.fi

Keywords

Biotransformation, cofactor recycling, cofactor regeneration, *Ralstonia eutropha*, *Cupriavidus necator*, hydrogen-oxidizing bacteria

Background

Biocatalysis is increasingly applied across different industries due to its efficiency and environmental benefits compared to chemical transformations. Biocatalysis using oxidoreductases often requires cofactors, such as nicotinamide nucleotides NADH and NADPH, but their stoichiometric addition to reaction mixtures is not economically feasible (1). Therefore, cofactor recycling systems are required. Traditionally cofactor recycling of NAD(P)H is performed using sacrificial substrates, such as glucose and formate, which are oxidized during the biocatalysis, while the cofactor is regenerated to its reduced form (2). This is not carbon-efficient, since D-gluconolactone and carbon dioxide (CO_2) are formed as by-products from glucose and formate, respectively. Specifically for the by-product D-gluconolactone, a substantial number of energy-rich electrons are wasted. In addition, glucose is produced by agriculture, which can decrease the overall sustainability of the production process due to, for example, competition with food production and environmental burdens of agriculture. Formate can be made from CO_2 and renewable electricity using electrochemical reduction. However, electrochemical production of formate has not yet been scaled-up and is not as energy-efficient as the electrochemical production of hydrogen (H_2) from water and electricity, which is already performed on a large scale (3).

H_2 is an attractive, byproduct-free sacrificial substrate for cofactor recycling. Molecular H_2 can be oxidized by organisms using hydrogenases. Some of the most extensively researched H_2-uptake hydrogenases are found in the hydrogen-oxidizing bacterium *Cupriavidus necator* H16 (formerly *Ralstonia eutropha*) (4). This bacterium possesses two types of hydrogenases that provide the cells with reducing power: membrane-bound and soluble hydrogenases (5). The membrane-bound hydrogenase is located in the cytoplasmic membrane where it directly feeds electrons to the respiratory chain for ATP production by oxidative phosphorylation. The NAD-dependent hydrogenase resides in the cytoplasm and is therefore referred to as soluble hydrogenase (SH) (6, 7). The electrons and protons from H_2 can be directly transferred to NAD^+ by the SH, reducing NAD^+ to NADH while simultaneously oxidizing hydrogen (4).

C. necator H16 SH has been researched broadly for cofactor recycling using purified enzymes (8-12). Compared to purified enzymes, whole-cell biocatalysts can provide enzyme stabilization, lower production cost and better inhibitor tolerance (13). In addition, cofactors are readily available inside the cells. Whole cells were used in one of the earliest studies of SH-catalyzed cofactor recycling in the 1980s where native *C. necator* cells reduced CO_2 to formate with a 30% yield (14). More recently, whole cells of recombinant *C. necator* have been employed as a biocatalyst by Oda et al. (15) and Assil-Companioni et al. (16) for reduction of hydroxyacetone to (*R*)-1,2-propanediol and for asymmetric C=C bond

reduction of unsaturated cyclic ketones, respectively. However, given the limited extent of research and number of products, further studies are required to investigate *C. necator* as a whole-cell biocatalyst. In the current study, we show that the scope of hydrogen-driven reductive bioconversions can be broadened to encompass a new class of products, sugar alcohols, with xylitol as a particular example.

Xylitol ($C_5H_{12}O_5$) is a sugar alcohol used widely as a sweetener (17). It is currently produced chemically from D-xylose ($C_5H_{10}O_5$), which is the second most abundant sugar in lignocellulosic biomass (18). The chemical production of xylitol requires extensively purified D-xylose to avoid inactivation of the catalyst. In contrast, biotechnological production does not have this requirement and exhibits greater tolerance for inhibitors. Many yeasts, along with some bacteria and filamentous fungi, naturally reduce D-xylose to xylitol (18). However, numerous studies have focused on heterologous expression of D-xylose reductase (XR), aiming to increase yield and productivity of xylitol (19-23). All these studies use sugars to power the conversion, and to our knowledge H_2 has not been used as the electron and energy source for the D-xylose-to-xylitol conversion.

The objective of this study was to develop a whole-cell biocatalyst strain of *C. necator* for xylitol production using H_2 as the electron donor. To achieve this, XR from *Scheffersomyces stipitis* (formerly *Pichia stipitis*) was expressed in *C. necator* to allow the cells to convert D-xylose into xylitol. The native SH of *C. necator* enabled the H_2-driven cofactor recycling required for bioconversion. Resting (i.e., non-dividing) cells were used in the experiments. These viable cells exhibit reduced metabolic activity, which allows energy to be directed towards bioconversion instead of biomass accumulation (24). With the experimental set-up used, we achieved nearly full quantitative conversions.

Materials and methods

Strains and culture media

Bacterial strains and plasmids used in this work are listed in Table 1 and the primers in Table S1 (see Additional file 1). *C. necator* H16 strains were grown in either rich BD BBL™ Trypticase™ Soy Broth (TSB) or minimal AUT medium (25) supplemented with 2 g/L fructose and glycerol (FG). Compared to the original AUT medium, the amount of $NiCl_2$ was doubled and SL-6 trace elements were added (1:1000) (26). *Escherichia coli* DH10β was used for plasmid construction. Tetracycline was added at a concentration of 10 µg/mL for *E. coli* and 5 µg/mL for *C. necator* when required. The sugars and sugar alcohols used in the study were purchased from Sigma-Aldrich.

56 **Table 1.** Bacterial strains and plasmids used in the study. The strains with △*phaC* deletion are unable to produce
57 polyhydroxybutyrate (PHB) for carbon and energy storage.

Strain	**Relevant characteristics**	**Source or reference**
C. necator H16 △*phaCAB*	△*phaC1* △*phaA1* △*phaB1*	(27)
C. necator H16 △*phaC1*	△*phaC1*	(28)
C. necator H16 △*A0006*	△*phaC1* △*A0006*	This study
C. necator H16 △*phaCAB*_gfp	△*phaCAB* derivative, pPj5:GFP	This study
C. necator H16 △*phaC*_gfp	△*A0006* derivative, pPj5:GFP	This study
C. necator H16 △*phaCAB*_xr	△*phaCAB* derivative, pPj5:XRsti	This study
C. necator H16 △*phaC*_xr	△*A0006* derivative, pPj5:XRsti	This study
Plasmid		
pLO3	Suicide vector, sacB	(29)
pLO3-*A0006*	pLO3 derivative with 1100 bp upstream and downstream regions of *A0006*	This study
pPj5:GFP	pSEVA521 containing Pj5 promoter and GFP	(30)
pPj5:XRsti	pPj5:GFP derivative, GFP replaced with D-xylose reductase from *Scheffersomyces stipitis* (XRsti)	This study

58

59 **Strain construction**

60 XR from *Scheffersomyces* (*Pichia*) *stipitis* was ordered codon-optimized for *C. necator* from GenScript (Additional file 1:
61 Table S2) and PCR amplified with Q5 High-Fidelity 2X Master Mix (NEB). The backbone plasmid pSEVA521+Pj5:GFP and
62 the amplified insert were digested with *Spe*I-HF and *Hin*dIII-HF (NEB) and ligated using T4 DNA ligase (NEB) to gain
63 pPj5:XRsti. The verified plasmid was transformed into electrocompetent *C. necator* cells. For preparing competent cells,
64 *C. necator* was grown in 100 mL of TSB supplemented with 20 mM of fructose to an optical density at 600 nm (OD_{600}) of
65 0.6 and washed twice with 1 mM $MgSO_4$. The pellet was resuspended into 2 mL of 1 mM MgSO4 and 1 mL of 60%
66 glycerol. Aliquots (50 µL) were stored in -80°C. Cells were mixed with plasmids (250 ng) in a 0.2 cm electroporation
67 cuvette (Bio-Rad), incubated 10 min on ice and electroporated with Electro Cell Manipulator ECM®630 (BTX) with the

68 following settings: 2.5 kV, 200Ω and 25µF. Super Optimal Broth with 20 mM fructose (950 µL) was added immediately
69 after electroporation and cells were incubated at 30°C and 180 rpm for 2-3 hours before plating on BBL™ Trypticase™
70 Soy Agar (TSA).

71 *C. necator* H16 △*A0006* was constructed from *C. necator* H16 △*phaC1* by deleting *A0006* with pLO3-based suicide vector
72 as previously described (29) (Additional file 1: Table S3). The △*A0006* restriction enzyme knockout increases
73 electroporation efficiency (31, 32) and is not expected to have any metabolic effects.

74 **XR activity assay**

75 For the XR activity assay, cells were grown overnight in TSB and then harvested by centrifugation (10 min, 2800 g). The
76 pellet was washed once with 50 mM potassium phosphate buffer (pH 7.5), resuspended into 1 mL of the same buffer
77 supplemented with cOmplete protease inhibitor (Roche) and moved into a 2 mL screw-cap tube with 400 µL of 0.5 mm
78 diameter glass beads. The cells were disrupted with FASTPREP-24 5G (MP Biomedicals) for 2x30sec at 6 m/s speed. After
79 disruption, the tube was centrifuged for 10 min at 16000 g, and the supernatant (soluble extract) was collected. Total
80 protein concentration was analyzed from the soluble extract by Quick Start™ Bradford Protein Assay (Bio-Rad) using
81 bovine serum albumin as the standard. XR activity assays were conducted in 96-well plates. The reaction mixture (330
82 µL) contained 0.15 mM of cofactor (NADH or NADPH), 50 mM potassium phosphate buffer (pH 6.0), 200 mM D-xylose
83 and an appropriate amount of soluble extract. Absorbance was measured at 340 mM using Epoch 2 Microplate
84 Spectrophotometer (BioTek). One unit of xylose reductase activity was defined as µmol of NAD(P)H oxidized per minute.
85 Specific activities were expressed as units per milligram of total protein. The results are given as averages of triplicate
86 assays.

87 **Bioconversions with resting cells**

88 Precultures were grown overnight in TSB media. FG media with tetracycline was inoculated to an initial OD_{600} of 0.1 and
89 grown for three days, reaching a final OD_{600} of approximately 4. The culture was centrifuged for 10 min at 2800 g and
90 washed twice with 100 mM sodium phosphate buffer (pH 7.0) to remove carbon and nitrogen sources. The cells were
91 resuspended in the same buffer with 30 g/L of substrate to an OD_{600} of 13-17, if not mentioned otherwise. This range of
92 OD_{600} corresponds approximately to a cell dry weight of 4.4-5.4 g/L. The prepared cell suspension (5 mL) was transferred
93 into an anaerobic serum bottle with a rubber stopper. D-xylose was the primary substrate, but one bioconversion was

also performed using L-arabinose and another using D-ribose. Three replicate bottles per bioconversion condition were prepared.

For the first bioconversion experiments, 100 mL serum bottles were filled with H_2 using vacuum-gas cycles to reach specific H_2 and oxygen (O_2) concentrations. As negative controls, bioconversions were performed under ambient air. The bottles were incubated at 30°C and 150 rpm. Samples (200 µL) were taken by opening the rubber stopper and the bottles were refilled with gasses after sampling. For bioconversion optimization, 50 mL serum bottles were filled with H_2 at the start of the bioconversion by flushing with 100% H_2 at 0.5 mL min^{-1} for 2 minutes. Samples (200 µL) were taken using a needle and syringe through the rubber stopper of sealed bottles. The approximate H_2 gas consumption was measured after bioconversions by filling a 50 mL syringe with air and recording the volume of air aspirated into the bottle through the syringe needle. Samples were centrifuged for 10 min at 16000 g and the supernatants were analyzed for sugars and sugar alcohols.

Calculation of H_2 consumption

The amount of H_2 consumed was calculated from the approximated H_2 gas consumption (Equation 1):

$$n\ (\mathrm{H_2\ consumed}) = \frac{pV}{RT} \quad (1)$$

where *p* is the pressure (0.98692 atm), *V* is the gas volume consumed (L), *R* is the gas constant (0.08206 L atm mol^{-1} K^{-1}) and *T* is the temperature (298.15 K).

One mole of H_2 is needed to reduce one mole of xylose (Equation 2):

$$\mathrm{H_2 + C_5H_{10}O_5 = C_5H_{12}O_5} \quad (2)$$

The total amount of xylitol produced was calculated as the sum of the xylitol at the end of the bioconversion and the xylitol in the fractions taken out during sampling. The ratio of xylitol production to H_2 consumption was calculated to determine the proportion of energy and protons transferred from H_2 to xylitol.

Analysis of sugars and sugar alcohols

Two different high performance liquid chromatography (HPLC) systems were used for D-xylose and xylitol analysis: Prominence-i LC-2030C (Shimadzu) equipped with Hi-Plex H 7.7x300 mm column (Agilent) at 45°C and 10 mM H_2SO_4 as eluent at a flow rate of 1 ml min^{-1} and Vanquish Flex (Thermo Fisher Scientific) equipped with Aminex Fast Acid Analysis

119 and HPX-87H columns (Bio-Rad) at 55°C and 2 mM H_2SO_4 as the eluent at a flow rate of 0.5 ml min^{-1}. An injection volume
120 of 10 µL was used in both HPLCs and the compounds were detected with a refractive index detector. L-arabinose, L-
121 arabitol, D-ribose and ribitol were analyzed with high pressure ion chromatography (HPIC) Dionex ICS-6000 (Thermo
122 Fisher Scientific) with CarboPac PA20 column (Thermo Fisher Scientific) at 30°C and 10 mM KOH as the eluent at a flow
123 rate of 0.5 ml min^{-1}. An injection volume of 2.5 µL was used and the compounds were detected with an electrochemical
124 detector. Conversion yields at specific time points were calculated by dividing the amount of xylitol by the total amount
125 of xylose and xylitol.

126 **Results**

127 **Xylose reductase from *S. stipitis* is functionally produced in *C. necator* H16**

128 In this study, two *C. necator* strains, △*phaC* and △*phaCAB*, with partial or full knockouts of the native pathway for storage
129 polymer polyhydroxybutyrate (PHB) formation, were used to avoid the accumulation of this by-product. Before
130 constructing the XR expressing strains, it was confirmed that the host strains cannot grow on C5 sugars and sugar
131 alcohols used in the study (Additional file 1: Fig. S1). Both strains were then transformed with the plasmids pPj5:XR,
132 carrying the codon-optimized XR from *S. stipitis,* and pPj5:GFP, as a negative control. Strains were cultivated
133 heterotrophically, and their soluble extracts were tested for XR activity. The soluble extracts of both XR strains showed
134 reductase activity with both NADPH and NADH cofactors, whereas no activity was detected in the negative control strains
135 (Table 2). Codon-optimized XR from *Candida parapsilosis* was also expressed in the host strains, but no activity was
136 detected (data not shown).

137 **Table 2.** Specific D-xylose reductase activities of soluble extracts with NADPH or NADH as cofactors (U/mg). The average
138 from three measurements is shown with the standard deviation. No activity could be detected in the negative controls.

Strain	**NADPH**	**NADH**
△*phaCAB*_xr	0.71±0.20	0.48±0.01
△*phaC*_xr	0.49±0.01	0.41±0.03

139

140 **Xylose is fully converted to xylitol by *C. necator* △*phaCAB***

141 The first bioconversion experiment was performed at 30 g/L D-xylose by both *C. necator* strains: △*phaCAB*_xr and
142 △*phaC*_xr. The suspensions were incubated under H_2 (85% H_2 + 15% air) or 100% ambient air. Under H_2, the

143 △*phaCAB*_xr strain reached complete bioconversion to xylitol within 16 days, whereas the △*phaC*_xr strain converted
144 78% of the provided D-xylose at the same time (Figure 1). Therefore, further bioconversions were performed using the
145 △*phaCAB*_xr strain. D-xylose was also converted to xylitol in the absence of H_2 by both strains, but the conversion yields
146 were under 25% after 16 days. This demonstrated successful cofactor recycling in resting cells of *C. necator* using H_2.

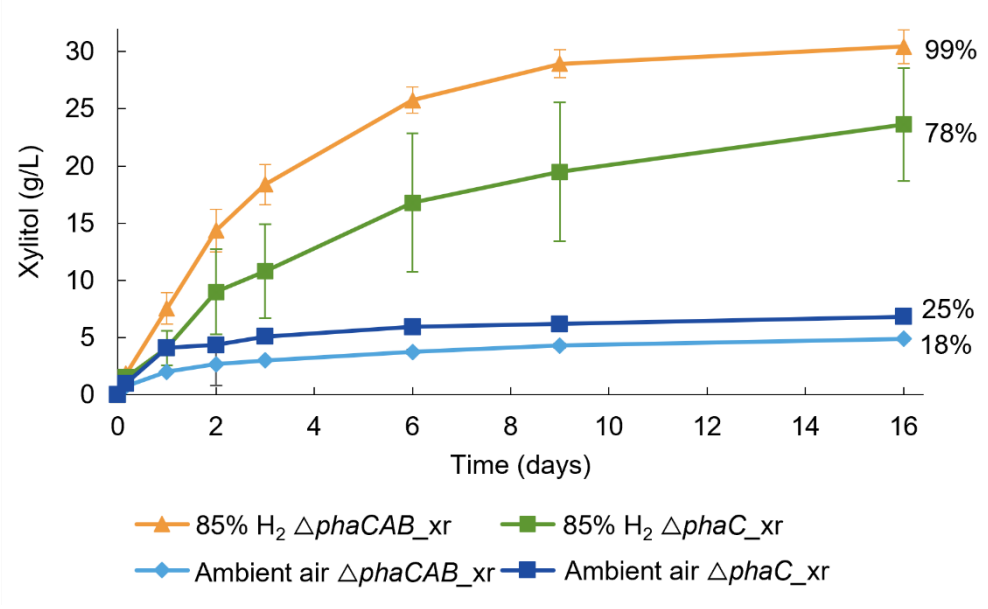

147

148 **Figure 1.** H_2-driven production of xylitol by *C. necator* △*phaCAB*_xr and △*phaC*_xr. The initial concentration of D-xylose
149 was 30 g/L in 100 mM sodium phosphate buffer (pH 7.0) with the cells at OD_{600} of 17 (△*phaCAB*_xr) and 15 (△*phaC*_xr).
150 The used gas mixture consisted of 85% H_2, 12% N_2, and 3% O_2 while ambient air contains 78% N_2 and 21% O_2. The average
151 from three bioconversions is shown with the standard deviation. The percentages represent the final yields.

152 **The oxygen concentration does not influence the bioconversion**

153 Since oxygen, acting as an electron acceptor, can provide the cells with energy via oxidative phosphorylation, we
154 examined the effect of oxygen concentration on the conversion rate. Three different oxygen concentrations (0, 1, and
155 4%) were tested. The conversion rates and yields showed little variation between the different oxygen concentrations
156 (Figure 2), with over 86% conversion yields being reached within 10 days in all conditions. After confirming that oxygen
157 was not a limiting factor, it was tested whether the amount of H_2 would be. Bioconversions with multiple H_2 flushes
158 during the experiment were compared to bioconversions with a single H_2 flush at the start. The results showed that
159 multiple H_2 flushes failed to improve the conversion yield (Additional file 1: Fig. S2). Therefore, further bioconversions
160 were conducted with only an initial H_2 flush.

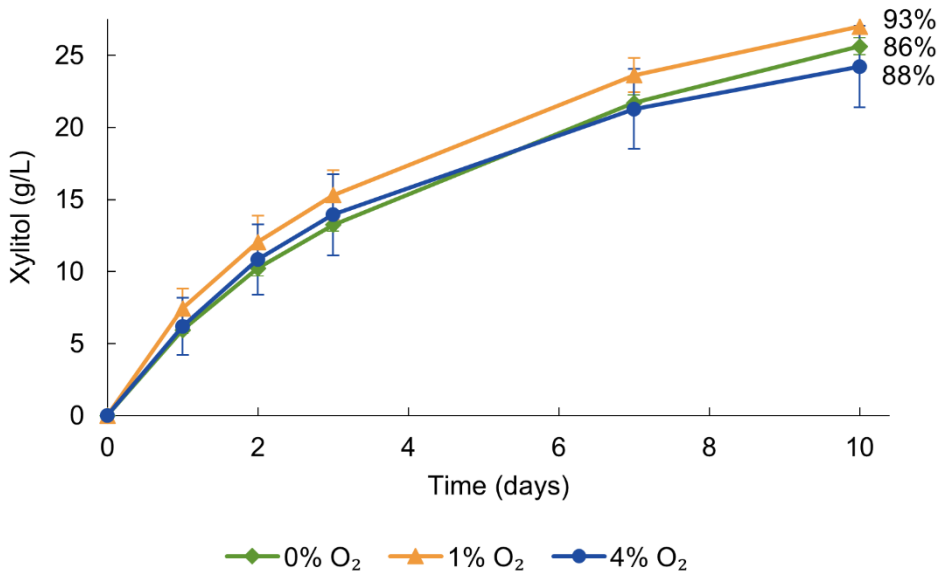

Figure 2. H_2-driven production of xylitol by *C. necator* △*phaCAB* on different oxygen concentrations. The reaction mixtures contained initially 30 g/L of D-xylose in 100 mM sodium phosphate buffer (pH 7.0) with cells at OD_{600} of 16. The used gas mixtures consisted of 0% O_2 and 100% H_2, 1% O_2, 2% N_2, and 97% H_2 or 4% O_2, 13% N_2, and 83% H_2. The average from three bioconversions is shown with the standard deviation. The percentages represent the final yields.

Higher initial sugar concentration can speed up the bioconversion rate

Four different D-xylose concentrations were tested to evaluate their impact on xylitol production rates. With increasing xylose concentration, the rate of conversion increased (Figure 3). The highest xylitol productivity in the first 48 hours (0.7 g L^{-1} h^{-1}) was reached with the highest xylose concentration used (114 g/L D-xylose). However, complete conversion was reached faster at a lower xylose concentration: 13 g/L of D-xylose was fully converted to xylitol in 10 days while 85% of 34 g/L D-xylose was converted within the same time.

In samples with the highest xylose concentrations (66 and 114 g/L), the final xylitol concentration reached 46 g/L. We hypothesized that H_2 in the headspace was limiting and that measuring H_2 consumption could allow us to estimate the electron conversion efficiency of hydrogen into xylitol. On average, 30 mL of gas was consumed under both conditions, equivalent to 1.2 mmol of H_2. Given that 0.2 mmol of xylitol was produced without H_2 (as shown in Figure 1) and 1.3 mmol was produced in total, it can be assumed that 1.1 mmol of xylitol was produced with the help of H_2 under both conditions. Consequently, more than 90% of the energy derived from H_2 was spent for the bioconversion, as one mole of H_2 is required to reduce one mole of xylose.

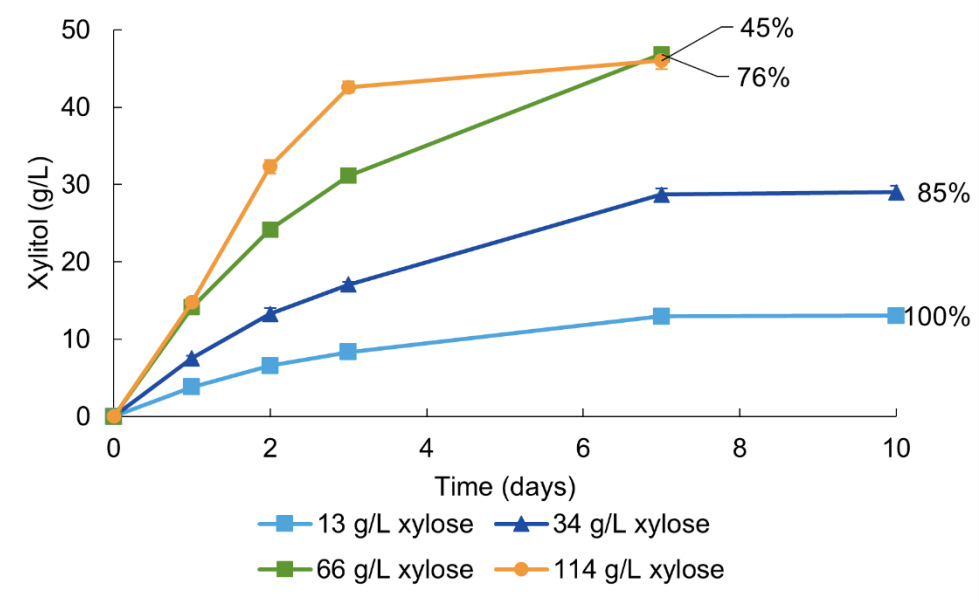

Figure 3. H_2-driven production of xylitol by *C. necator* △*phaCAB* at different D-xylose concentrations. The reaction mixtures were composed of 13, 34, 66, and 114 g/L of D-xylose in 100 mM sodium phosphate buffer (pH 7.0) and cells at OD_{600} of 13-15. The headspace contained 100% H_2. The average from three bioconversions is shown with the standard deviation. The percentages represent the final yields.

Increased cell concentration enhances the rate of bioconversion

So far, all bioconversions in this study were conducted with a cell concentration range of OD_{600} 13-17. The effect of the amount of the whole-cell biocatalyst was examined at lower and higher cell concentrations: OD_{600} 7 and 60. With the highest cell concentration, full conversion of 30 g/L D-xylose to xylitol was achieved in 7 days (Figure 4). Increasing the cell concentration had a positive effect also on the xylitol production rate. In the first 24 hours, the production rates were 0.5 g L^{-1} h^{-1} and 0.1 g L^{-1} h^{-1} for the highest and lowest cell concentrations used, respectively.

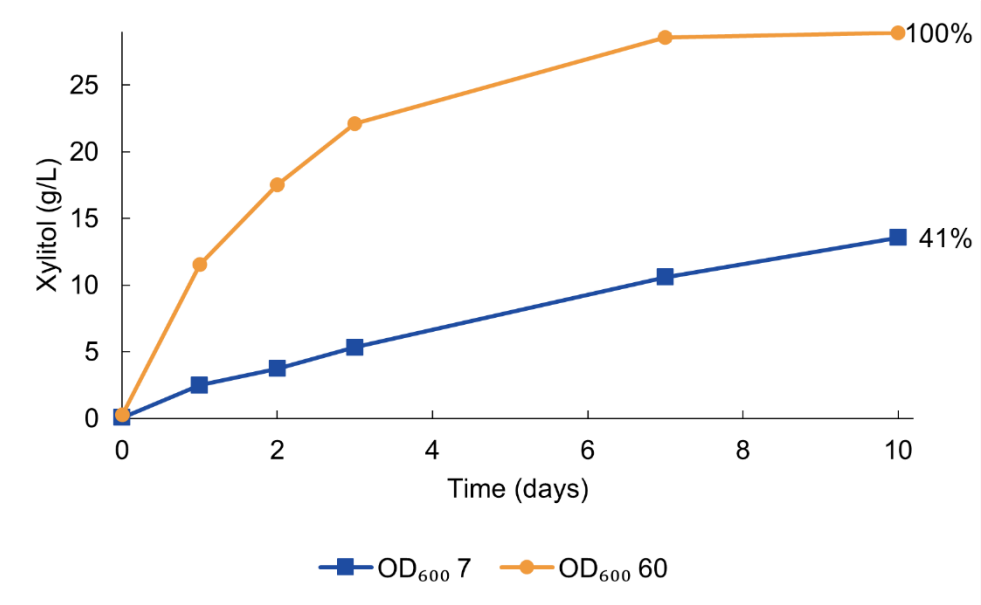

190

191 **Figure 4.** H_2-driven production of xylitol by *C. necator* △*phaCAB* at different cell concentrations. The initial concentration
192 of D-xylose was 30 g/L. The conversions were carried out in a 100 mM sodium phosphate buffer (pH 7.0) under 100%
193 H_2. The average from three bioconversions is shown with the standard deviation. The percentages represent the final
194 yields.

195 **Arabinose and ribose are reduced to sugar alcohols by the resting cells**

196 *S. stipitis* XR is also known to convert L-arabinose and D-ribose into their respective sugar alcohols (33). Therefore, we
197 examined whether *C. necator* harboring the xylose reductase could also be used as a biocatalyst for these conversions.
198 Both sugars were successfully reduced to their corresponding sugar alcohols, with the production rates and yields of L-
199 arabitol and ribitol being only slightly lower than those for xylitol (Figure 5).

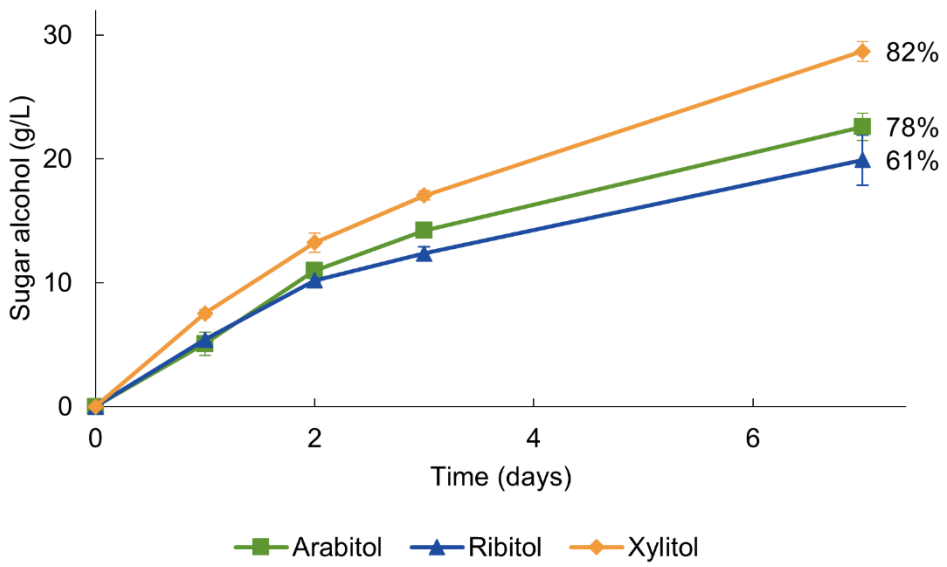

200

201 **Figure 5.** H_2-driven production of L-arabitol, ribitol and xylitol by C. necator △*phaCAB*. The initial concentrations of L-
202 arabinose, D-ribose and D-xylose were 28, 30 and 34 g/L, respectively, and the corresponding cell densities (OD_{600}) were
203 15, 15, and 13. The experiments were carried out in a 100 mM sodium phosphate buffer (pH 7.0) under 100% H_2. The
204 average from three bioconversions is shown with the standard deviation. The percentages represent the final yields.

205 **Discussion**

206 This study aimed to advance the development of *C. necator* as a H_2-driven whole-cell biocatalyst. We demonstrated a
207 full reduction of 30 g/L of D-xylose to xylitol in resting cells using H_2 for cofactor regeneration. The effects of different
208 parameters on xylitol production were studied to improve the production rates. Up to 30 g/L of xylitol was produced in
209 *C. necator* △*phaCAB_xr* within 7 days and 100% conversion yield (Figure 4). Additionally, it was shown that the system
210 can also convert L-arabinose and D-ribose into their respective sugar alcohols (Figure 5).

211 *C. necator* accumulates polyhydroxybutyrate (PHB) as a carbon and energy storage compound. To avoid this
212 accumulation, which could also lead to cofactor oxidation, PHB-negative strains △*phaCAB* and △*phaC* of *C. necator* were
213 used as hosts. Comparison of the △*phaCAB*_xr *and* △*phaC*_xr strains revealed that deletion of the whole PHB pathway
214 (*phaCAB*) enhanced both the bioconversion rate and yield (Figure 1). In the △*phaC* knock-out strain, it is possible that
215 some of the reducing equivalents from H_2 were consumed by the NAD(P)H-utilizing acetoacetyl-CoA reductase (PhaB)
216 of the PHB pathway. The advantage of knocking out more than just the *phaC* gene has also been observed in earlier
217 studies in non-resting cells of *C. necator*. For instance, complete deletion of the PHB pathway was found to be beneficial

218 for resveratrol production in *C. necator,* whereas deletion of only the *phaC* gene did not improve the titer compared to
219 the wild type (34).

220 Oxygen is essential for ATP production from H_2 in *C. necator*. Although the bioconversion reaction itself does not require
221 ATP, it was hypothesized that the cells would require some ATP for cell maintenance. However, the results suggest
222 otherwise (Figure 2). This outcome is advantageous for industrial applications, as oxygen-free production mitigates the
223 risk associated with flammability of H_2-O_2 mixtures. The experiments also demonstrated efficient transfer of nearly all
224 hydrogen-derived electrons into the product. When enough H_2 was present in the headspace, full bioconversion of
225 xylose could be demonstrated. However, liquid solubility of H_2 is low and hence may still limit the rate of conversion. To
226 test this, bioconversions could be performed under elevated pressure, where H_2 solubility is increased, but
227 unfortunately it was not possible to test this with the current experimental set-up. Additionally, mass transfer of H_2 to
228 the liquid phase can be significantly improved by using optimized bioreactors equipped with specialized gas spargers
229 and impellers (35).

230 The most significant improvements in the bioconversion rate were achieved by increasing the cell concentration and
231 xylose concentration. This is not surprising, as a higher cell concentration provides more catalyst for the conversion to
232 occur, and an increased substrate concentration boosts the reaction rate until enzyme saturation is reached. The most
233 efficient xylitol production systems reported in the literature have reached higher xylitol productivity than the 0.7 g L^{-1}
234 h^{-1} achieved in this study. At a similar cell density, recombinant *E. coli* cells, coexpressing a D-xylose reductase and a
235 glucose dehydrogenase, produced xylitol at 6.4 g L^{-1} h^{-1}. In this optimized process, a 100% yield was achieved at an initial
236 D-xylose concentration of 200 g/L using glucose for cofactor recycling (23). Factors that could account for this include
237 lower enzyme activities, slower substrate and product transport into and outside of the cell, and particularly the
238 aforementioned poor H_2 solubility. Observing the SDS-PAGE gel of Jin et al., it seems that their XR level in the cell was
239 much higher than in this study (Additional file 1: Fig. S3). Although the strongest promoter currently known for *C. necator*
240 was used in the present study (30, 36), stronger expression of XR could improve the bioconversion rates. The expression
241 systems for *C. necator* need further development to achieve the expression levels obtained with *E. coli*. On the other
242 hand, the xylose and xylitol transport systems of *E. coli* are likely more efficient than those of *C. necator* because *E. coli*
243 can natively grow on xylose whereas *C. necator* cannot. A BLAST search of the *C. necator* H16 genome using the D-xylose
244 specific transport systems of *E. coli* (XylE and XylFGH) yielded no matches, suggesting that *C. necator* lacks xylose-specific
245 transporters. Xylose is likely transported into the cells by a sugar transporter with side activity for xylose. Hence,

246 heterologous introduction of a xylose transporter could be considered for future studies to further improve
247 bioconversion rates.

248 The specific activity of XR with NADPH was higher compared to NADH (Table 2). The same result has been observed
249 previously by Verduyn, Van Kleef (33). Using NADPH-producing SH, instead of the native NADH-producing SH, with
250 NADPH-dependent oxidoreductases could increase the rate of the bioconversion. The NAD^+-specific SH from *C. necator*
251 has been engineered to also accept $NADP^+$, but its $NADP^+$-reducing activity would need to be increased (12). Another
252 option is to use NADH-preferring oxidoreductases or to engineer them to have this preference, ensuring high activity
253 towards NADH.

254 This article presented the first whole-cell, H_2-driven biocatalysis study using a PHB-negative *C. necator* strain as the host.
255 Direct comparison of this work to the few prior studies is challenging due to differences in experimental setups, product
256 types, enzyme kinetics, and strains used. Oda et al. (15) reported a productivity of 0.9 g L^{-1} h^{-1} for (*R*)-1,2-propanediol,
257 which is within the same order of magnitude as our findings. Whole-cell cofactor recycling using SH has not only been
258 done in *C. necator*. Lonsdale et al. (37) expressed SH from *C. necator* in *Pseudomonas putida* to perform H_2-driven
259 bioconversion of n-octane to 1-octanol. The cofactor recycling proved to be effective, resulting in a threefold increase
260 in 1-octanol production in the presence of H_2. However, the yield and rate of bioconversions they achieved were
261 significantly lower than the ones in this study; Lonsdale et al. reported a maximum productivity of 0.01 g L^{-1} h^{-1}, about
262 100-fold lower than the rates we and Oda et al. achieved.

263 The limited amount of research in this area offers a wide range of opportunities for improving these organisms to
264 perform H_2-driven bioconversions towards industrial applications. Bioconversion rates can likely be significantly
265 improved using hosts with improved enzyme activities, elevated pressures, higher cell concentrations and optimized
266 bioreactor designs that enhance hydrogen solubility.

267 **Conclusions**

268 Cofactor recycling via hydrogenases represents a promising alternative for traditional bioconversion systems because of
269 its atom efficiency, lack of by-products and the prospects of H_2 becoming a renewable platform chemical of the future.
270 This study demonstrated H_2-driven bioconversion of D-xylose to xylitol in XR expressing *C. necator* strain. 30 g/L of D-
271 xylose was fully converted into xylitol in 7 days. It was shown that nearly all the energy from H_2 is harnessed by the

bioconversion, demonstrating the potential of the *C. necator* system as an efficient H_2-driven biocatalyst for sugar alcohol production and potentially other products.

Data availability

The datasets generated and analyzed during the current study are available from the corresponding author on reasonable request.

Competing interests

The authors declare that they have no competing interests.

Funding

This work was supported by the Research Council of Finland (KNALLRED—Hydrogen powered reductive biosyntheses and biotransformations by an engineered Knallgas bacterium, grant number 342124).

Authors' contributions

All authors designed research. TJ conducted experiments, data analysis, and wrote the manuscript. All authors revised and approved the manuscript.

Acknowledgements

The authors thank Enrico Orsi for the *C. necator* △*phaCAB* strain, Guillermo Bordanaba Florit for constructing the *C. necator* H16 △*A0006* strain, Victor de Lorenzo's lab for the SEVA plasmid, and Ton van Gelder for the help with HPLC analyses. We also thank Solar Foods, especially Juha-Pekka Pitkänen, for the fruitful discussions and the bioeconomy research infrastructures of Aalto University for the support.

Additional file 1: Table S1. Oligonucleotide primers used in the study. **Table S2.** Synthesized xylose reductase gene used in this study originating from *Scheffersomyces stipitis*. **Table S3.** Upstream and downstream regions of *A0006* used to create *C. necator* H16 △*A0006*. **Figure S1.** The growth of *C. necator* strains △*phaCAB* and △*phaC* on different sugars and sugar alcohols (100 mM). **Figure S2.** Comparison of bioconversion with a single H_2 flush at the start and H_2 flush after every sampling. **Figure S3.** SDS-PAGE analysis of soluble extracts by *C. necator* H16 strains.

296 **References**

297 1. Wang X, Saba T, Yiu HHP, Howe RF, Anderson JA, Shi J. Cofactor NAD(P)H Regeneration
298 Inspired by Heterogeneous Pathways. Chem. 2017; doi:10.1016/j.chempr.2017.04.009
299 2. van der Donk WA, Zhao H. Recent developments in pyridine nucleotide regeneration. Curr
300 Opin Biotechnol. 2003; doi:10.1016/s0958-1669(03)00094-6
301 3. Stöckl M, Claassens NJ, Lindner SN, Klemm E, Holtmann D. Coupling electrochemical CO_2
302 reduction to microbial product generation - identification of the gaps and opportunities. Curr Opin
303 Biotechnol. 2022; doi:10.1016/j.copbio.2021.11.007
304 4. Lubitz W, Ogata H, Rudiger O, Reijerse E. Hydrogenases. Chem Rev. 2014;
305 doi:10.1021/cr4005814
306 5. Lenz O, Lauterbach L, Frielingsdorf S, Friedrich B. Oxygen-tolerant hydrogenases and their
307 biotechnological potential. In: Rögner M, editor. Biohydrogen. Berlin: Walter de Gruyter GmbH; 2015.
308 6. Jugder BE, Chen Z, Ping DT, Lebhar H, Welch J, Marquis CP. An analysis of the changes in soluble
309 hydrogenase and global gene expression in *Cupriavidus necator* (*Ralstonia eutropha*) H16 grown in
310 heterotrophic diauxic batch culture. Microb Cell Fact. 2015; doi:10.1186/s12934-015-0226-4
311 7. Cramm R. Genomic view of energy metabolism in *Ralstonia eutropha* H16. J Mol Microbiol
312 Biotechnol. 2009; doi:10.1159/000142893
313 8. Holzer AK, Hiebler K, Mutti FG, Simon RC, Lauterbach L, Lenz O, et al. Asymmetric Biocatalytic
314 Amination of Ketones at the Expense of NH_3 and Molecular Hydrogen. Org Lett. 2015;
315 doi:10.1021/acs.orglett.5b01154
316 9. Ratzka J, Lauterbach L, Lenz O, Ansorge-Schumacher MB. Systematic evaluation of the
317 dihydrogen-oxidising and NAD^+-reducing soluble [NiFe]-hydrogenase from *Ralstonia eutropha* H16 as a
318 cofactor regeneration catalyst. Biocatal Biotransform. 2011; doi:10.3109/10242422.2011.615393
319 10. Al-Shameri A, Willot SJ, Paul CE, Hollmann F, Lauterbach L. H_2 as a fuel for flavin- and H_2O_2-
320 dependent biocatalytic reactions. Chem Commun. 2020; doi:10.1039/d0cc03229h
321 11. Cha J, Bak H, Kwon I. Hydrogen-fueled CO_2 reduction using oxygen-tolerant oxidoreductases.
322 Front Bioeng Biotechnol. 2022; doi:10.3389/fbioe.2022.1078164
323 12. Preissler J, Reeve HA, Zhu T, Nicholson J, Urata K, Lauterbach L, et al. Dihydrogen-Driven
324 NADPH Recycling in Imine Reduction and P450-Catalyzed Oxidations Mediated by an Engineered O_2-Tolerant
325 Hydrogenase. ChemCatChem. 2020; doi:10.1002/cctc.202000763
326 13. Lin B, Tao Y. Whole-cell biocatalysts by design. Microb Cell Fact. 2017; doi:10.1186/s12934-
327 017-0724-7
328 14. Klibanov AM, Alberti BN, Zale SE. Enzymatic synthesis of formic acid from H_2 and CO_2 and
329 production of hydrogen from formic acid. Biotechnol Bioeng. 1982; doi:10.1002/bit.260240104
330 15. Oda T, Oda K, Yamamoto H, Matsuyama A, Ishii M, Igarashi Y, et al. Hydrogen-driven
331 asymmetric reduction of hydroxyacetone to (R)-1,2-propanediol by *Ralstonia eutropha* transformant
332 expressing alcohol dehydrogenase from *Kluyveromyces lactis*. Microb Cell Fact. 2013; doi:10.1186/1475-
333 2859-12-2
334 16. Assil-Companioni L, Schmidt S, Heidinger P, Schwab H, Kourist R. Hydrogen-Driven Cofactor
335 Regeneration for Stereoselective Whole-Cell C=C Bond Reduction in *Cupriavidus necator*. ChemSusChem.
336 2019; doi:10.1002/cssc.201900327
337 17. da Silva S, Chandel A. D-Xylitol: Fermentative production, application and commercialization.
338 1st ed. Heidelberg: Springer-Verlag; 2012.
339 18. Narisetty V, Cox R, Bommareddy R, Agrawal D, Ahmad E, Pant KK, et al. Valorisation of xylose
340 to renewable fuels and chemicals, an essential step in augmenting the commercial viability of lignocellulosic
341 biorefineries. Sustain Energ Fuels. 2022; doi:10.1039/d1se00927c
342 19. Hallborn J, Walfridsson M, Airaksinen U, Ojamo H, Hahn-Hägerdal B, Penttilä M, et al. Xylitol
343 production by recombinant *Saccharomyces cerevisiae*. Nat Biotechnol. 1991; doi:10.1038/nbt1191-1090
344 20. Nyyssölä A, Pihlajaniemi A, Palva A, von Weymarn N, Leisola M. Production of xylitol from D-
345 xylose by recombinant *Lactococcus lactis*. J Biotechnol. 2005; doi:10.1016/j.jbiotec.2005.03.014

21. Cirino PC, Chin JW, Ingram LO. Engineering *Escherichia coli* for xylitol production from glucose-xylose mixtures. Biotechnol Bioeng. 2006; doi:10.1002/bit.21082

22. Sasaki M, Jojima T, Inui M, Yukawa H. Xylitol production by recombinant *Corynebacterium glutamicum* under oxygen deprivation. Appl Biochem Biotechnol. 2010; doi:10.1007/s00253-009-2372-2

23. Jin LQ, Xu W, Yang B, Liu ZQ, Zheng YG. Efficient Biosynthesis of Xylitol from Xylose by Coexpression of Xylose Reductase and Glucose Dehydrogenase in *Escherichia coli*. Appl Biochem Biotechnol. 2019; doi:10.1007/s12010-018-2878-0

24. Julsing MK, Kuhn D, Schmid A, Buhler B. Resting cells of recombinant *E. coli* show high epoxidation yields on energy source and high sensitivity to product inhibition. Biotechnol Bioeng. 2012; doi:10.1002/bit.24404

25. Lenz O, Lauterbach L, Frielingsdorf S. O_2-tolerant [NiFe]-hydrogenases of *Ralstonia eutropha* H16: Physiology, molecular biology, purification, and biochemical analysis. Methods Enzymol. 2018; doi:10.1016/bs.mie.2018.10.008

26. Atlas RM. Handbook of Microbiological Media. 4th ed. Washington DC: Taylor & Francis; 2010.

27. Collas F, Dronsella BB, Kubis A, Schann K, Binder S, Arto N, et al. Engineering the biological conversion of formate into crotonate in *Cupriavidus necator*. Metab Eng. 2023; doi:10.1016/j.ymben.2023.06.015

28. Lütte S, Pohlmann A, Zaychikov E, Schwartz E, Becher JR, Heumann H, et al. Autotrophic production of stable-isotope-labeled arginine in Ralstonia eutropha strain H16. Appl Environ Microbiol. 2012; doi:10.1128/AEM.01972-12

29. Lenz O, Friedrich B. A novel multicomponent regulatory system mediates H_2 sensing in *Alcaligenes eutrophus*. Proc Natl Acad Sci. 1998; doi:10.1073/pnas.95.21.12474

30. Claassens NJ, Bordanaba-Florit G, Cotton CAR, De Maria A, Finger-Bou M, Friedeheim L, et al. Replacing the Calvin cycle with the reductive glycine pathway in *Cupriavidus necator*. Metab Eng. 2020; doi:10.1016/j.ymben.2020.08.004

31. Xiong B, Li Z, Liu L, Zhao D, Zhang X, Bi C. Genome editing of *Ralstonia eutropha* using an electroporation-based CRISPR-Cas9 technique. Biotechnol Biofuels. 2018; doi:10.1186/s13068-018-1170-4

32. Vajente M, Clerici R, Ballerstedt H, Blank LM, Schmidt S. Using *Cupriavidus necator* H16 to provide a roadmap for increasing electroporation efficiency in non-model bacteria. bioRxiv. 2024; doi:10.1101/2024.05.27.596136

33. Verduyn C, Van Kleef R, Frank J, Schreuder H, Van Dijken JP, Scheffers WA. Properties of the NAD(P)H-dependent xylose reductase from the xylose-fermenting yeast *Pichia stipitis*. Biochem J. 1985; doi:10.1042/bj2260669

34. Jang Y, Lee YJ, Gong G, Lee SM, Um Y, Kim KH, et al. Carbon dioxide valorization into resveratrol via lithoautotrophic fermentation using engineered *Cupriavidus necator* H16. Microb Cell Fact. 2024; doi:10.1186/s12934-024-02398-x

35. Tanaka K, Ishizaki A, Kanamaru T, Kawano T. Production of poly(D-3-hydroxybutyrate) from CO_2, H_2, and O_2 by high cell density autotrophic cultivation of *Alcaligenes eutrophus*. Biotechnol Bioeng. 1995; doi:10.1002/bit.260450312

36. Gruber S, Hagen J, Schwab H, Koefinger P. Versatile and stable vectors for efficient gene expression in *Ralstonia eutropha* H16. J Biotechnol. 2014; doi:10.1016/j.jbiotec.2014.06.030

37. Lonsdale TH, Lauterbach L, Honda Malca S, Nestl BM, Hauer B, Lenz O. H_2-driven biotransformation of n-octane to 1-octanol by a recombinant *Pseudomonas putida* strain co-synthesizing an O_2-tolerant hydrogenase and a P450 monooxygenase. Chem Commun. 2015; doi:10.1039/c5cc06078h

Additional file 1

H_2-driven xylitol production in *Cupriavidus necator* H16

Tytti Jämsä[1,*], Nico J. Claassens[2], Laura Salusjärvi[1], Antti Nyyssölä[1]

[1] VTT Technical Research Centre of Finland Ltd., Tekniikantie 21, 02150 Espoo, Finland

[2] Laboratory of Microbiology, Wageningen University, Stippeneng 4, 6708WE Wageningen, the Netherlands

*Correspondence to Tytti Jämsä: tytti.jamsa@vtt.fi

399 **Table S1**. Oligonucleotide primers used in the study.

Primer	5' to 3' sequence	Details
oXR1	CCCAAGCTTTTAAAAGGGGAGGTATTTCTATGCCGTCGATCAAGCTGAA	PCR of synthesized *S. stipitis* XR for cloning
oXR2	CTAGACTAGTACCCCTTCCTTACACGAAGA	PCR of synthesized *S. stipitis* XR for cloning
oSEVA_F	TCTAGGGCGGCGGAT	Colony PCR
oSEVA_R	CTGGATTCTCACCAATAAAAAACG	Colony PCR

400

401 **Table S2.** Synthesized xylose reductase gene used in this study originating from *Scheffersomyces stipitis*.
402 Codon-optimized for *C. necator* (957 bp). The original sequence is associated with GeneID 4839234.

Name	Nucleotide sequence
XRsti	ATGCCGTCGATCAAGCTGAACTCGGGCTACGACATGCCGGCCGTGGGCTTCGGCTGCTGG AAGGTGGACGTGGACACCTGCTCGGAACAGATCTACCGCGCCATCAAGACCGGCTACCGC CTGTTCGACGGCGCCGAGGACTACGCCAACGAAAAGCTGGTGGGCGCCGGCGTGAAGAAG GCCATCGACGAGGGCATCGTGAAGCGCGAAGACCTGTTCCTGACCTCGAAGCTGTGGAAC AACTACCACCACCCGGACAACGTGGAGAAGGCCCTGAACCGCACCCTGAGCGACCTGCAG GTGGACTACGTGGACCTGTTCCTGATCCACTTCCCGGTGACCTTCAAGTTCGTGCCGCTG GAGGAAAAGTACCCGCCGGGCTTCTACTGCGGCAAGGGCGACAACTTCGACTACGAGGAC GTGCCGATCCTGGAAACCTGGAAGGCCCTGGAGAAGCTGGTGAAGGCCGGCAAGATCCGC TCGATCGGCGTGTCGAACTTCCCCGGCGCCCTGCTGCTGGACCTGCTGCGCGGCGCAACC ATCAAGCCGTCGGTGCTGCAGGTGGAACACCACCCGTACCTGCAGCAGCCGCGCCTGATC GAGTTCGCCCAGAGCCGCGGCATCGCCGTGACCGCCTACTCGAGCTTCGGCCCGCAGTCG TTCGTGGAGCTGAACCAGGGCCGCGCCCTGAACACCAGCCCGCTGTTCGAGAACGAAACC ATCAAGGCCATCGCCGCCAAGCACGGCAAGAGCCCGGCCCAGGTGCTGCTGCGCTGGTCG AGCCAGCGCGGCATCGCCATCATCCCGAAGTCGAACACCGTGCCGCGCCTGCTGGAAAAC AAGGACGTGAACAGCTTCGACCTGGACGAGCAGGACTTCGCCGACATCGCCAAGCTGGAC ATCAACCTGCGCTTCAACGACCCGTGGGACTGGGACAAGATCCCGATCTTCGTGTAA

403

404 **Table S3.** Upstream and downstream regions of *A0006* used to create *C. necator* H16 △*A0006.*

Description	5’ to 3’ sequence
Upstream of *A0006*	CAAAGCTGGGCCGGATGCTGTGCGTGCTGCTGAAGGCGAAACGATACTGCTGTGGGACGG TTCGAACGCTGGGGAATTCTTCAGGTCCAAGGTCGGGTTGGTTGCTTCGACGATGACGAA GATTTCTCCGAGCAGTGTTTTTCGTCCGGCATACTTTTTTCATGTCGCCAAGCAAGCTGA GCGATTCCTGAAGGCTCAAACCAATGGCACTGGCATTCCACACGTTGACCGAGAGCTTCT CGAGGGGATAAAGGTCTTTTGTCCTGGCTCTACGGAGCAGCAATTACTTGCGGAAATCCT CGACACTCTCGACACCGCCATCTACGAAACTGAAGCGATCATCGCCAAGCTCAAGGCGGT CAAGCAAGGCCTGCTGCATGACCTCTTGACGCGCGGCATCGACGCCAACGGCGAATTGCG CCCACCTCAGGCCGAGGCACCGCATCTCTACGAGTCGTCACCGTTGGGTTGGATTCCGAA TGAGTGGGGTCTTGCTCCTACAGCAACTCGCTGCCATCTGATAACCAAAGGCACTACCCC TGCGGCTAATGAGATGTGGCAGGGTGGCGCGGGAATTAGGTTTCTGCGAGTCGATAATCT TTCTTTCGATGGACAACTGGATCTAGATGCAAGCACGTTTCGAGTTAGCCTTGCCACGCA CAAAGGTTTTCTGGCTCGTTCAAGATGCCTTGAAGGTGATGTGCTGACGAACATCGTTGG CCCACCTCTAGGGAAACTGGGGCTTGTTACCAAAGAAATTGGTGAGGTCAATATTAATCA AGCAATTGCGTTATTTCGACCAACCGAACAACTACTGCCAAAGTTCCTATTAATCTGGCT TAGTAGCTCAATCTCGCAGTCTTGGCTGAGGAACCGAGCCAAGCAGACGTCGGGACAAGT GAATCTGACCCTCGCTCTATGCCAGGAGCTTCCTCTACCTCGGATGACGATCAATGAGCA ACAGGCAATCGTTGACCGAGTTGATGCCGCGCAGGAACAAATCTGGTGTGAGGAGGAACT GATCCGAAAGATGCGACTTGAGAAATCTGGCCTTATGGATGACCTCCTCACCGGCCGCGT CCGCGTCAAGCCGCAGCTGGCGGAAACCAAACAAGCAGGGAGCGCCTGATG
Downstream of *A0006*	GCGCCTGATGCACGACAAGCTGATGCAGGTGTGATTCGATGCCTTCGCCGGTGAAATTGC CAAGCCTTCAGATCGGTGACCTCCGGTTCACGCTCCAGCGGAGCGCGCGCCGCAGAACTA TGCAGATCACCGTGGAGCGCAGTGGCGACTTGATGCTCTGCGCACCGCCGGAGGTGGACG AGGCCGCGCTGCGAGCATTCGTGCTGGAGAAGCGCTTCTGGATCTACACCAAGCTGGCCG AGAAGGACCGCTTGCAGCGCCAGGTTCCGCGCAAGGAATTCGTCGGAGGCGAGGGATTCT TGTATCTCGGCCGCAGCCATCGGCTGAAGGTGGTCGATGAACAGAATGTGCCACTGAAGT TGAATGGAGGCCGCTTTTGTCTGCGCCGTGACGCCCTACCCGCCGCGCGCGAGCATTTCA TCCGCTGGTACGGCGAGCGTGCCAAGGCCTGGCTTTCGGGGCGTGTAGCTGACTACCAGT CGCGAATGGAGGTGACGCCTGCCGGCGTCAAGGTGCAGGACCTTGGATATCGCTGGGGTT CGTGTGGCAAGGGCGACTGGCTGTACTTCCACTGGAAGGCAATCCTGCTGCCGGCGCGCA TCGCTGAGTATGTCGTGGTGCATGAGATTGCCCATCTGCATGAGCCGCACCACACGCCTG CGTTCTGGCTTCGAGTGGAGCGTGCCATGCCGGACTATGCGCAACGCAAGGCCTGGCTGG CCGAGCATGGAATCGATGTTGAAGGAATCTAAAGAACGATGGCTGACTATTTCACCAGTG ACTACTTCAAGCTGCTGAACAAGTGGAAGGGGCAGAAGCGTGACGAGTCCAACCCCGAGC AGAACCGCGCTTATGAAGATCTGAAGAAGGCCTACGAGGTGACGGAGGCGTGGGCGGACA AGGTTAAGGCCGAGTTGTTCCCTGTCGGGCGCGTCGAGATTCGTAAGCGCCCGACCAACC AGGGCAACAACTTTGCCAGCTACAACTGGGCCAAAATCTACCCTTCATCTGAGGCGCCGA AAGAGTTGGCTTACACAGTTGGCATCGGCGCCGATGACGGCTTCGTAGTCAAGATCGATA CCGTTGGGCTCGACGAATTGGACGCGACGAGAAAGGCCTAT

405

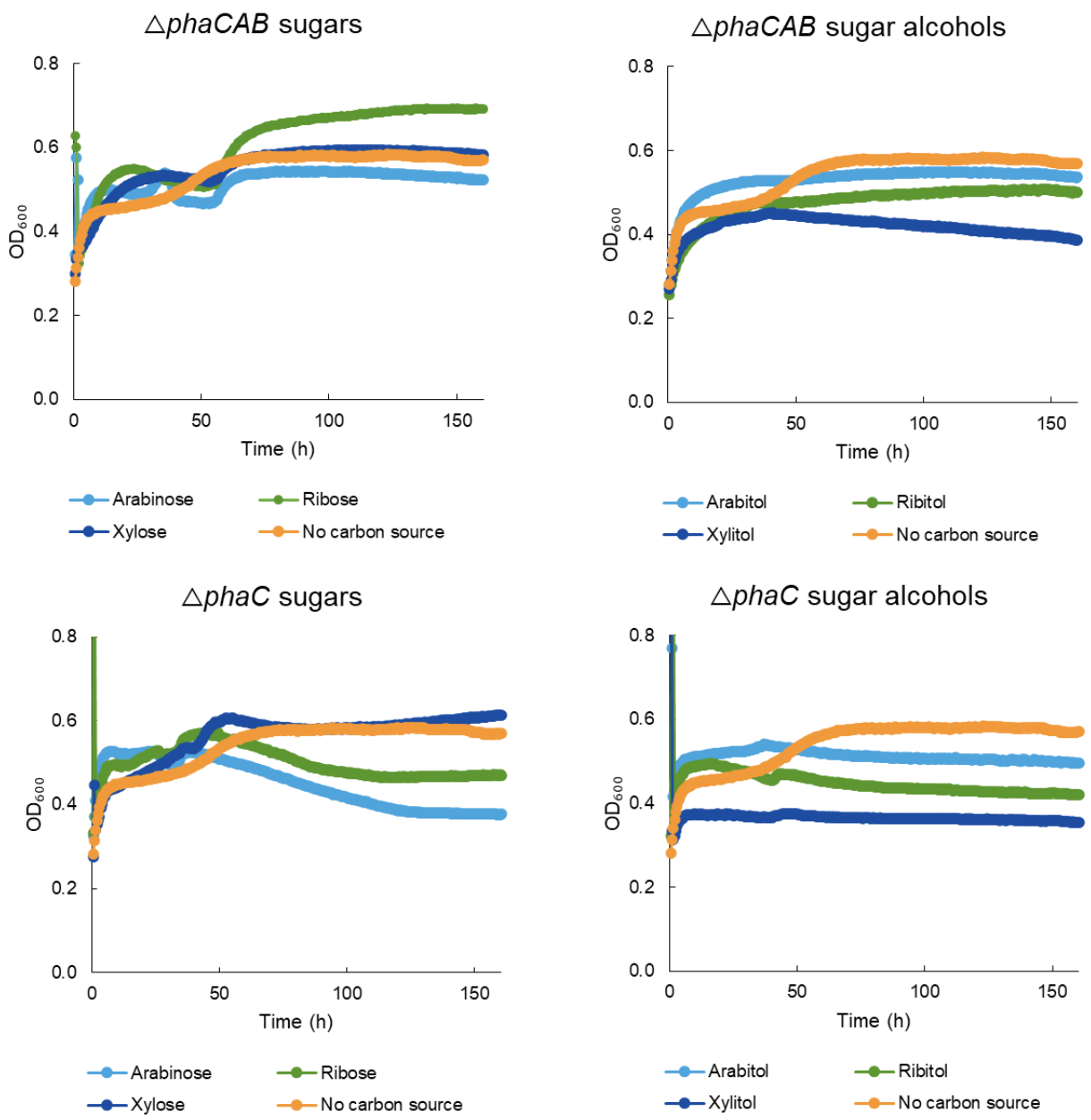

Figure S1. The growth of *C. necator* strains △*phaCAB* and △*phaC* on different sugars and sugar alcohols (100 mM). Precultures were grown in TSB. Cells were cultivated in 96-well plate at an initial OD_{600} of 0.05 in 130 µl of AUT media supplemented with the carbon sources. The cultures were topped with 50 µl of mineral oil to avoid evaporation. The negative control was cultivated in AUT media without any carbon source. The 96-well plate was incubated at 30°C using a double shake orbital at 282 rpm. All conditions had three replicates.

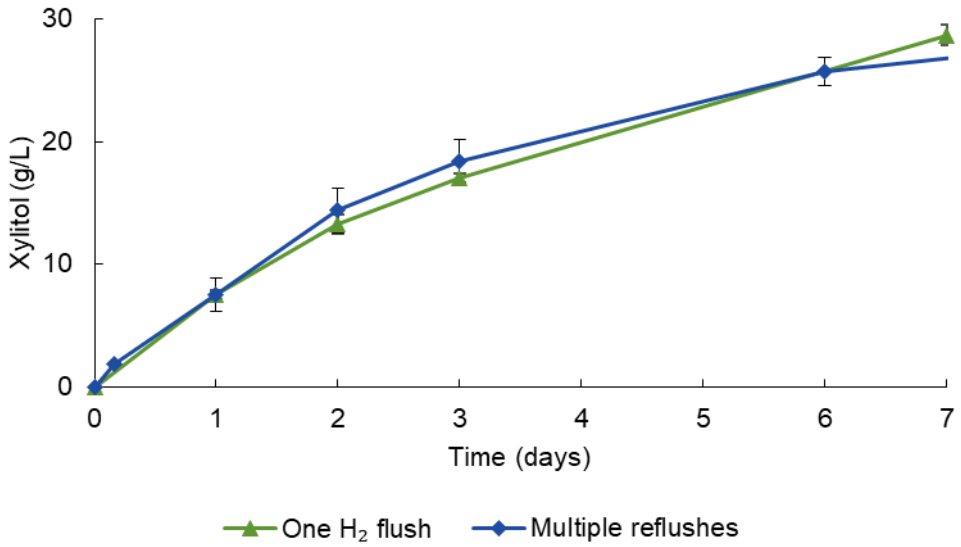

412

413 **Figure S2**. Comparison of bioconversion with a single H_2 flush at the start and H_2 flush after every sampling.
414 The initial concentration of D-xylose was 34 g/L (one H_2 flush) and 30 g/L (multiple reflushes) in 100 mM
415 sodium phosphate buffer (pH 7). The cell concentrations were OD_{600} of 13 (one H_2 flush) and OD_{600} of 17
416 (multiple reflushes).

417

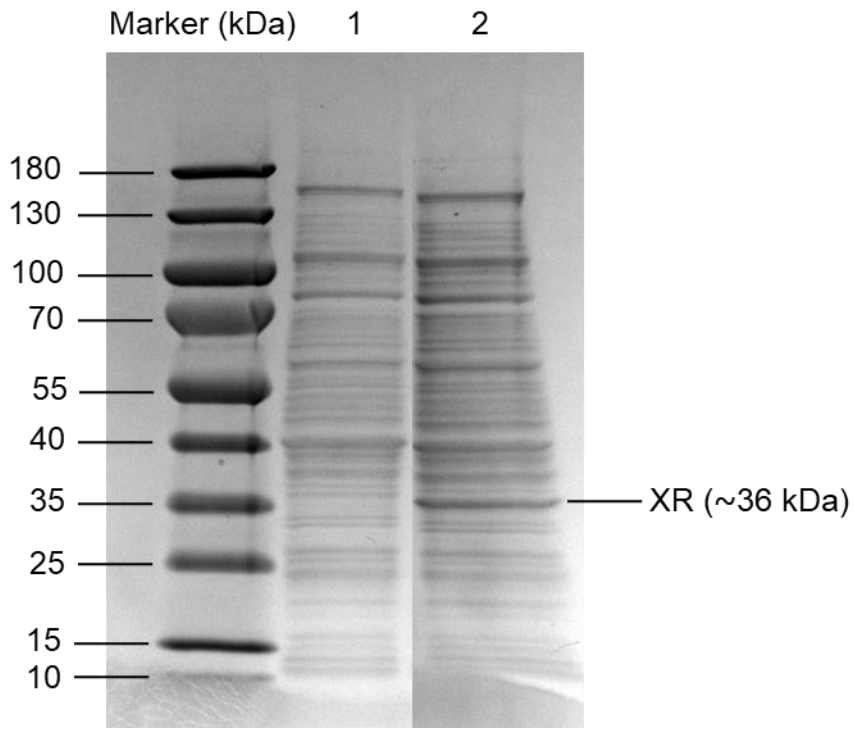

418

419 **Figure S3.** SDS-PAGE analysis of soluble extracts by *C. necator* H16 strains. Lane 1, wild type *C. necator* H16.
420 Lane 2, △*phaCAB*_xr (△*phaCAB* with XRsti under Pj5 promoter).

421